

Breaking the Memory Wall for Heterogeneous Federated Learning with Progressive Training

Yebo Wu

University of Macau
State Key Lab of IoTSC
yc37926@um.edu.mo

Chunlin Tian

University of Macau
State Key Lab of IoTSC
yc27402@um.edu.mo

Li Li*

University of Macau
State Key Lab of IoTSC
llili@um.edu.mo

Chengzhong Xu

University of Macau
State Key Lab of IoTSC
czxu@um.edu.mo

ABSTRACT

Federated learning (FL) enables multiple devices to collaboratively train a shared model while preserving data privacy. Existing FL approaches usually assume that the global model can be trained on any participating devices. However, in real-world cases, a large memory footprint during the training process bottlenecks the deployment on memory-constrained devices. This paper presents **ProFL**, a novel progressive FL framework to effectively break the memory wall. Specifically, ProFL divides the model into different blocks based on its original architecture. Instead of updating the full model in each training round, ProFL first trains the front blocks and safely freezes them after convergence. Training of the next block is then triggered. This process iterates until the training of the whole model is completed. In this way, the memory footprint is effectively reduced for feasible deployment on heterogeneous devices. In order to preserve the feature representation of each block, we decouple the whole training process into two stages: progressive model shrinking and progressive model growing. During the progressive model shrinking stage, we meticulously design corresponding output modules to assist each block in learning the expected feature representation and obtain the initialization parameters. Then, the obtained output modules are utilized in the corresponding progressive model growing stage. Additionally, to control the training pace for each block, a novel metric from the scalar perspective is proposed to assess the learning status of each block and determines when to trigger the training of the next one. Finally, we theoretically prove the convergence of ProFL and conduct extensive experiments on representative models and datasets to evaluate the effectiveness of ProFL. The results demonstrate that ProFL effectively reduces the peak memory footprint by up to 57.4% and improves model accuracy by up to 82.4%.

KEYWORDS

Federated Learning, On-Device Training, Limited Memory Capacity

1 INTRODUCTION

Federated Learning (FL) is a new learning paradigm that enables multiple devices to collaboratively train a global model while preserving data privacy. Most existing algorithms operate under the assumption that the participating devices possess sufficient memory capacity to train the global model [32] [34] [26]. However, in real-world scenarios, the participating clients, such as smartphones and wearable devices, usually have limited resources. For instance, training ResNet50 [13] on ImageNet [7] with a batch size of 128 requires 26GB of memory. On the contrary, the available memory on the commonly used mobile devices typically only ranges from 4 to 16GB [16]. Moreover, to obtain high analysis capability, current models are becoming deeper and wider, leading to an even higher memory footprint. Such constraint prevents the deployment of FL on mobile devices in real-world cases. On the other hand, only training the small model that can fit the existing devices leads to low model representation capability and limits the application scope of FL.

To surmount the resource limitation of the participating devices, several works have been proposed. The existing work can be mainly divided into the following two categories: 1) model-heterogeneous FL and 2) partial training. The approaches in the first category employ the local model tailored to match the memory capacity of each participating device [20] [17] [6]. Knowledge distillation [14] is then performed for model aggregation. However, a public dataset is required to complete the information transfer between different model architectures, which is usually hard to retrieve due to privacy concerns in real-world cases. For the second category, the methods include both width scaling [9] [1] [15] and depth scaling [18] [24]. For width scaling, the corresponding approach scales the channels of convolutional layers to resize the model size, thus accommodating clients' available memory capacity. However, this approach substantially compromises the model's architecture and introduces challenges related to channel mismatch during aggregation [18], thus struggling to effectively leverage information from low-memory devices. For depth scaling, clients can train models of different depths based on their memory constraints. However, this method has a strong assumption that some of the participating clients can afford to train the full model during the local training process. The models that can be trained are still bounded by the

high-end devices. Thus, a new training paradigm that can effectively break through the memory limitation of the participating devices to conduct high-performance training without a public dataset is crucial for FL in real-world deployment.

In this paper, we propose ProFL, a novel progressive training approach that breaks the memory wall of FL from a new perspective. Unlike vanilla Federated Learning, which continuously updates the full model throughout the whole learning process, ProFL employs a well-designed progressive training paradigm, training only a portion of the model in each round and progressively completing the training of the full model. First, it divides the model into different blocks, allowing clients who can afford the training of the current block to participate. Then, when the current block converges, this block is frozen, and a new block is added for training on top of it. In this way, the backpropagation process of the frozen part and the corresponding memory space for storing the intermediate activations are effectively saved. This process iterates continuously until all blocks have been successfully trained. As the memory footprint during the training process is notably reduced, devices with heterogeneous hardware configurations can be involved in the training procedure.

ProFL mainly consists of the following two stages: 1) progressive model shrinking and 2) progressive model growing. Progressive model shrinking is designed to construct corresponding output modules and acquire the initialization parameters for each block. During the training process of each block, except for the last block, which has an output module for end-to-end training, the other blocks lack the ability to undergo independent training. Simply adding a fully connected layer can severely compromise the feature representation of each block, as each block aims to extract different levels of features in the original model [5]. To tackle this challenge, we utilize convolutional layers to replace each subsequent block, mimicking the position of the training block in the original model and preserving their position information. Specifically, we first train each block of the model from back to front and integrate the trained block information into a convolutional layer. Through this process, we obtain convolutional layers carrying block-specific information for building output modules. At the same time, we acquire the initialization parameters for each block, resulting in better optimization results. Then, the retrieved output modules and initialization parameters are utilized during the training process of each block, the progressive model growing stage.

Furthermore, block freezing determination is designed to evaluate the training progress of each block, safely freeze it after convergence and then trigger the training of the next block. Specifically, we propose a new metric from the scalar perspective to accurately assess the convergence status of each block. This metric captures the updated status of each scalar by analyzing its movement distance. Initially, high gradients drive effective movement toward the optimal solution. As training advances, diminishing gradients lead to reduced scalar movement distance. Ultimately, scalar oscillation at the optimal solution results in near-zero movement distance within a window, signifying convergence. We sum movement distances of all scalars within a block, termed effective movement, as a measure of block training progress. This metric facilitates accurate tracking of individual block learning progress, allowing safe initiation of block freezing without compromising model performance.

To the best of our knowledge, ProFL is the *first* work that breaks the memory wall of FL and resolve the restriction of client’s memory capacity on the global model to be trained.

In summary, our main contributions are as follows: (1) We propose ProFL, a novel FL approach that effectively breaks the memory wall through progressive block training. We decouple model training into progressive model shrinking and progressive model growing to assist each block in learning the expected feature representation. (2) To accurately evaluate the training progress of each block, we delve into the scalar perspective and introduce a novel metric named effective movement. (3) We theoretically prove the convergence of ProFL and conduct extensive experiments to validate its superiority on representative models and datasets.

2 RELATED WORK

In order to make the low-end devices participate in the learning process, the following two main categories of training methodologies have been proposed: 1) model-heterogeneous FL and 2) partial training.

Model-Heterogeneous FL. Model-heterogeneous FL is designed to relax the resource constraints of the mobile clients, in which different models are deployed on the central server and the participating clients. For instance, FedMD [20] customizes models with varying complexities for each client. After completing local training, the clients upload logits on a public dataset to the server. The server then aggregates the uploaded logits and conducts training on the public dataset, facilitating information transfer. Similar approaches include FedDF [23], DS-FL [17], and Fed-ET [6]. However, these methods require a public dataset, which is typically not feasible in real-world cases due to privacy issues. Although some algorithms, such as FedZKT [39], generate a public dataset using GAN [11], the training of GAN is often unstable, which deteriorates the performance of the global model.

Partial Training. Partial training only trains part of the model by performing width scaling or depth scaling. HeteroFL [9] is a representative width scaling method, where convolutional layers are scaled to match devices with varying available memory capacity. Similar methods include Federated Dropout [4] and FjORD [15]. However, these methods may significantly disrupt the model’s architecture, leading to performance degradation. Consequently, scaling the model from the depth perspective has been proposed. For instance, DepthFL [18] customizes models with different depths based on client memory constraints. However, the global model size in DepthFL is constrained by the device with the largest memory capacity. Motivated by this, we propose ProFL, a progressive training framework that gradually reduces memory requirements by intelligently freezing earlier layers. This framework facilitates training a larger global model than the largest client model.

3 PROFL

Considering an FL system with N clients, each client has a local dataset, denoted as D_n (where $1 \leq n \leq N$). ProFL is designed to efficiently train a model Θ based on the memory-limited devices. Fig. 1 represents the overall workflow of ProFL. ProFL first divides the global model into T blocks based on the model architecture. Subsequently, distinct sub-models are constructed for each training step, forming the model shrinking pool and model growing pool. At each step, the client set S is selected from the pool of clients who can

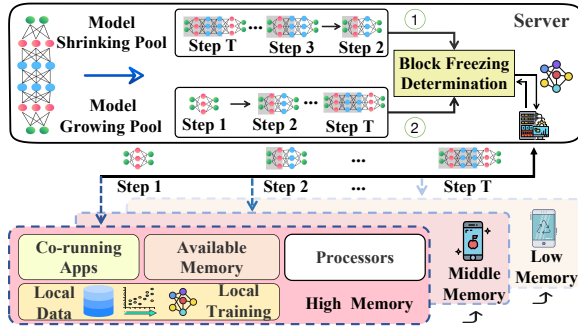


Figure 1: Workflow of ProFL. Divide the model into different blocks, obtaining a *Model Shrinking Pool* and a *Model Growing Pool*. First, **progressive model shrinking is performed, followed by progressive model growing, and Block Freezing Determination is used to evaluate the training status of each step’s sub-model.** Simultaneously, select devices for training based on the available memory. In this figure, each layer is considered as a block, and the gray part in the model represents the parameters of this layer are frozen.

afford training for the current block. After that, the training process is triggered, ProFL initially performs progressive model shrinking by sequentially training each block of the model from back to front and integrating the information from each trained block into a convolutional layer. The purpose of this stage is twofold: 1) obtaining the initialization parameters for each block and, 2) constructing the corresponding output modules for the progressive model growing using the obtained convolutional layers. Then, ProFL initiates progressive model growing by gradually expanding the model from the first block until each block has undergone sufficient training, ultimately achieving the target model. Throughout both the progressive model shrinking and progressive model growing stages, the training pace of each step is controlled by the block freezing determination to efficiently determine whether the current block has been well trained, safely freeze it and trigger the next training step.

Section 3.1 elaborates on the progressive training paradigm. To further enhance model performance, we introduce progressive model shrinking in Section 3.2. Section 3.3 elucidates how the block freezing determination controls the training pace of each step. Finally, in Section 3.4, we theoretically prove the convergence of ProFL.

3.1 Progressive Training Paradigm

In this section, we introduce the progressive training paradigm, namely, the progressive model growing as shown in Fig. 2. The global model Θ to be trained can be divided into T blocks $[\theta_1, \theta_2, \dots, \theta_T]$. The block being actively trained is represented as θ_t ($1 \leq t \leq T$), the frozen block as $\theta_{t,F}$, and the well-trained block as θ_t^* . The sub-model of the t -th step during progressive model growing is denoted as $\Theta_t = [\theta_{1,F}^*, \theta_{2,F}^*, \dots, \theta_t]$. When $1 \leq t < T$, the sub-models at each step cannot independently undergo end-to-end training due to the absence of output modules. To facilitate this progressive training process, it is essential to add an output module θ_{op} to each training block. Consequently, the model trained at step t can be represented as $\Theta_t = [\theta_{1,F}^*, \theta_{2,F}^*, \dots, \theta_t, \theta_{op}]$. Once the current block converges, it

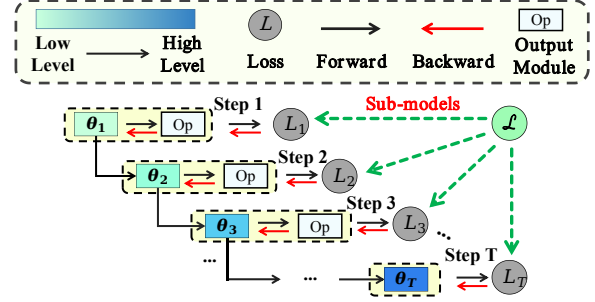


Figure 2: Progressive Model Growing. *Low Level* and *High Level* represent different levels of image features.

advances to step $t + 1$. This process iterates until the overall global model is well trained.

In this step-wise progressive training paradigm, each round is performed as follows: 1) The central server determines the sub-model Θ_t^r ($[\theta_{1,F}^*, \theta_{2,F}^*, \dots, \theta_t, \theta_{op}]$) of the current round r to be trained; 2) Select the client set S and send Θ_t^r to them; 3) The selected clients train Θ_t^r on their local datasets. Since the previous blocks are frozen, only parameters $[\theta_t, \theta_{op}]$ are updated; 4) After completing local training, the updated parameters ($[\theta_{t,n}^r, \theta_{op,n}^r]$, where $n \in S$) are uploaded to the central server; 5) The central server then aggregates parameters according to Eq. (1) and replace the updated parameters at their respective positions to obtain Θ_t^{r+1} .

$$[\theta_{t,g}^r, \theta_{op,g}^r] = \sum_{n \in S} \frac{|D_n|}{|D|} ([\theta_{t,n}^r, \theta_{op,n}^r]) \quad (1)$$

where $|D_n|$ represents the size of local dataset on client n , $|D|$ represents the amount of the overall training data, $[\theta_{t,n}^r, \theta_{op,n}^r]$ stand for the updated model parameters of client n on round r , and $[\theta_{t,g}^r, \theta_{op,g}^r]$ represent the aggregated global model parameters. Following parameter aggregation, the block freezing determination assesses the training progress of the current block. If the current block is well trained, it safely freezes it and triggers the next training step. Upon convergence of the current block, we obtain θ_t^* . The model for the next step $t + 1$ is derived by introducing a new block θ_{t+1} based on the blocks trained in the preceding t steps, represented as $\Theta_{t+1} = [\theta_{1,F}^*, \theta_{2,F}^*, \dots, \theta_t^*, \theta_{t+1}, \theta_{op}]$.

However, the progressive training paradigm encounters two primary challenges. The first challenge revolves around constructing corresponding output modules θ_{op} to aid each block in learning the expected feature representation. Inappropriately constructed output modules can significantly impact the final model performance. To address this challenge, we employ progressive model shrinking (Section 3.2) before progressive model growing. This process facilitates obtaining convolutional layers with block-specific information for constructing output modules and acquiring the initialization parameters for each block. The second challenge pertains to controlling the training pace of each block. As highlighted in [35], improper freezing may adversely affect the final model performance. In response, we introduce a novel metric (Section 3.3) to assess the training progress of each block, ensuring judicious freezing for optimal results.

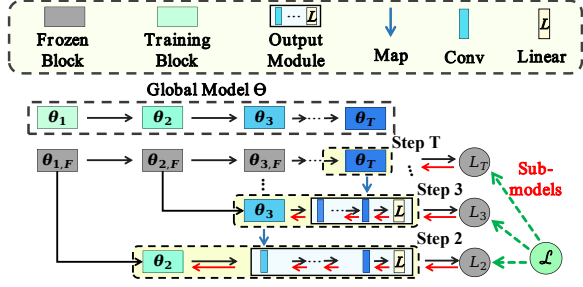


Figure 3: Progressive Model Shrinking. Progressive model shrinking builds the required output modules and obtains initialization parameters for each block. *Map* implies integrating the information learned by the block into a convolutional layer.

3.2 Progressive Model Shrinking

Fig. 3 shows the overall workflow of progressive model shrinking, it transforms the model in the opposite direction, serving two primary purposes. Firstly, the parameters obtained by training each block from back to front are utilized to initialize the corresponding block in the progressive model growing stage. Secondly, following the training of each block, information from the block is integrated into a convolutional layer, acting as a component of the output module, guiding blocks in learning their expected feature representation. Information integration is completed through knowledge distillation [14]. The resulting convolutional layers, in conjunction with a fully connected layer, collectively form the output module θ_{op} . In specific, the convolutional layer corresponding to block t is denoted as $\theta_{t,Conv}$ and the fully connected layer is denoted as θ_L . As illustrated in Fig. 3, the output module used in each step of progressive model shrinking corresponds to the one applied in each step of progressive model growing.

The distinction between progressive model shrinking and progressive model growing in each round of the training process is as follows: 1) For step t during progressive model shrinking, the sub-model is represented as $\Theta_t = [\theta_{1,F}, \theta_{2,F}, \dots, \theta_t, \theta_{t+1,Conv}, \dots, \theta_{T,Conv}, \theta_L]$, undergoing continuous training until block θ_t converges, yielding θ_t^{ini} . It is worth noting that, during the training process of each step, only the current block and the output module are updated. This significantly reduces the computational load of both forward and backward propagation, minimizing training overhead, and effectively reduces memory footprint. 2) Fig. 3 illustrates that, upon convergence, the information from block θ_t^{ini} is integrated into a convolutional layer $\theta_{t,Conv}$, and a new output module θ_{op} ($[\theta_{t,Conv}, \theta_{t+1,Conv}, \dots, \theta_{T,Conv}, \theta_L]$) for model Θ_{t-1} is constructed. Subsequently, it proceeds to step $t-1$ and initiates the training of θ_{t-1} . These two steps are iteratively performed until the second block completes training and integrates its information into the corresponding convolutional layer. After completing this stage, we can obtain the initialization parameters for each block and convolutional layers with block-specific information to construct the output modules.

3.3 Block Freezing Determination

The block freezing determination is deployed on the server side to assess the training progress of each block, safely freeze it and trigger

the training of the next block. Layer freezing [35] [3] [22] is widely adopted in centralized training to expedite model training and mitigate computational costs. However, the existing approaches cannot be directly applied to the FL scenario. For instance, Egeria [35] uses a reference model for assessing layer convergence, relying on the raw training data, which are not accessible for privacy concerns in FL. To precisely evaluate the training progress of each block, we introduce a novel metric from the scalar perspective. This metric directs during both progressive model shrinking and progressive model growing stages.

Specifically, we define the update of a scalar s at the k -th epoch as $U_s^k = s^k - s^{k-1}$, and $\|U_s^k\|$ represents the movement distance of the scalar. Consequently, the absolute movement distance of this scalar over H consecutive epochs can be expressed as $D_{s,k}^H = \|\sum_{h=0}^{H-1} U_s^{k-h}\|$. As a parameter tends to converge, $D_{s,k}^H$ approaches 0. The rationale behind this lies in the fact that when the gradient is relatively large at the outset, the scalar swiftly moves in the direction of the optimal solution, and this movement direction remains consistent within the window size H , thus resulting in a relatively large absolute movement distance. As training proceeds, the gradient decreases, leading to a reduction in the movement distance. When the scalar is in proximity to the optimal solution, it oscillates near this point, causing the movement distance under the window H to approach 0.

The movement distance of all parameters within a block can be expressed as $D_{B,k}^H = \sum_{s \in B} D_{s,k}^H$, indicating the overall update of the block. A larger $D_{B,k}^H$ signifies that all scalars in the block are actively moving towards the optimal point. Conversely, if $D_{B,k}^H$ is smaller, it suggests that all parameters in the block are near the optimum point, indicating that the block is approaching convergence. Considering the varying parameter quantities and update scales across different blocks and different scalars, we normalize $D_{B,k}^H$ by dividing it by $\sum_{s \in B} \sum_{h=0}^{H-1} \|U_s^{k-h}\|$. The resulting normalized value $\frac{D_{B,k}^H}{\sum_{s \in B} \sum_{h=0}^{H-1} \|U_s^{k-h}\|}$ is defined as effective movement, providing insight into the learning status of the block. Therefore, we evaluate the training progress of each block by calculating its effective movement. We use linear least-squares regression [36] to fit the effective movement and analyze the slope to determine the optimal freezing time. If the slope is continuously below threshold ϕ for W evaluations, we freeze the current block and proceed to the next step.

3.4 Convergence Analysis

In this section, we prove the convergence of the freezing-based progressive training paradigm based on [12]. While prior works have demonstrated the convergence of partial training [27], the key difference lies in their neglect of memory constraints. Consequently, in proving convergence, they solely focus on assessing the similarity of gradients between sub-models and the global model. Unlike them, we freeze the well-trained blocks at each step. For example, in step t , we exclusively train the parameters θ_t of the model Θ_t . Without loss of generality, we omit the output module here.

Notation. Let f_1, \dots, f_N represent local functions, M_t be the total number of every device's SGDs on step t and E be the number of local epochs. Assuming \mathbf{x} and \mathbf{y} are any two points in the function's

domain. When training neural networks, our goal is to find the optimal global model parameters Θ^* that minimizes the empirical loss $f: \mathbb{R}^d \rightarrow \mathbb{R}$: $f^* := \min_{\Theta \in \mathbb{R}^d} f(\Theta)$.

Assumption 1 (μ -strongly convex). For any arbitrary \mathbf{x} and \mathbf{y} , there exists:

$$f_n(\mathbf{x}) - f_n(\mathbf{y}) \geq (\mathbf{x} - \mathbf{y})^T \nabla f_n(\mathbf{y}) + \frac{\mu}{2} \|\mathbf{x} - \mathbf{y}\|_2^2, \forall \mathbf{x}, \mathbf{y}, n \quad (2)$$

Assumption 2 (L -smooth). The functions $f_1, \dots, f_N: \mathbb{R}^d \rightarrow \mathbb{R}$ is differentiable and there exists a constant $L > 0$ such that:

$$f_n(\mathbf{x}) - f_n(\mathbf{y}) \leq (\mathbf{x} - \mathbf{y})^T \nabla f_n(\mathbf{y}) + \frac{L}{2} \|\mathbf{x} - \mathbf{y}\|_2^2, \forall \mathbf{x}, \mathbf{y}, n \quad (3)$$

This ensures that the gradient cannot change arbitrarily fast. [25] indicates that this is a weak assumption practically guaranteed in most machine learning models, such as logistic regression, deep neural networks, etc.

Assumption 3 (Bounded stochastic gradient variance). Let $\xi_{t,n}^m$ be sampled from the n -th device's local data uniformly at random. For any $\Theta_{t,n}^m \in \mathbb{R}^d$, we can obtain bounded stochastic gradient variance [40] [38] [30] [31] [21]. For any $t \in \{1, 2, \dots, T\}$ and $m \in \{1, 2, \dots, M_t\}$, there exists parameters $\sigma_{t,n}^2 \geq 0$ that satisfies:

$$\mathbb{E} \|\nabla f_n(\Theta_{t,n}^m, \xi_{t,n}^m) - \nabla f_n(\Theta_{t,n}^m)\|^2 \leq \sigma_{t,n}^2, \forall t, n, m \quad (4)$$

When $t = 1$, signifying an individual model is undergoing end-to-end training. This assumption transforms into the standard assumption for analyzing the convergence of Stochastic Gradient Descent (SGD). When $t \neq 1$ the step-wise sub-model Θ_t is constructed by adding θ_t to the model Θ_{t-1} .

Assumption 4 (Uniform stochastic gradient). The expected squared norm of stochastic gradients is uniformly bounded [12] [30] [31], i.e., $\mathbb{E} \|\nabla f_n(\Theta_{t,n}^m, \xi_{t,n}^m)\|^2 \leq G^2$ for all $n = 1, \dots, N$, $t = 1, \dots, T$ and $m = 1, \dots, M_t - 1$.

Assumption 1 formally establishes a fundamental lower bound crucial for ensuring the convergence of the loss function to a stationary point [21]. It implies that a globally optimal solution Θ^* is guaranteed to exist. Assumptions 2-4 are standard stochastic optimization assumptions [12] [30] [31]. Utilizing the above standard assumptions, we first prove the convergence of the model at $t = 1$ and then extend it to the model at $t \neq 1$.

Theorem 1. Let Assumptions 1, 2, 3 and 4 hold and $L, \mu, \sigma_{t,n}, G$ be defined therein. Let $\kappa = \frac{L}{\mu}$, $\gamma = \max\{8\kappa, E\}$, $C = \frac{4}{|S|} E^2 G^2$ and the stepsize $\eta_m = \frac{2}{\mu(\gamma+m)}$. Assuming $f^*(\Theta_t)$ and $f_n^*(\Theta_t)$ are the minimum values of $f(\Theta_t)$ and $f_n(\Theta_t)$ respectively, and p_n is the aggregation weight for device n , the data heterogeneity degree is expressed as $\Gamma = f^*(\Theta_t) - \sum_{n=1}^N p_n f_n^*(\Theta_t)$. Then:

$$\mathbb{E}[f(\Theta_t^{M_t})] - f^*(\Theta_t) \leq \frac{\kappa}{\gamma + M_t - 1} \left(\frac{2(B+C)}{\mu} + \frac{\mu\gamma}{2} \mathbb{E} \|\Theta_t^1 - \Theta_t^*\|^2 \right), \quad (5)$$

where $B = \sum_{n=1}^N p_n^2 \sigma_{t,n}^2 + 6L\Gamma + 8(E-1)^2 G^2$. It can be seen that, for strongly convex and smooth functions, as well as Non-IID data, FedAvg converges to the global optimum at a rate of $\mathcal{O}(\frac{1}{M_t})$. When $t = 1$, Eq. (5) simplifies to the standard convergence proof for end-to-end model training in FL. When $t \neq 1$, due to the freezing of the preceding blocks, their exclusive function is to map the data from a low-dimensional space to a high-dimensional space. Therefore, when training the subsequent blocks, it is still equivalent to training

an end-to-end model. The difference between this freezing-based progressive training framework and end-to-end training is that model training is broken down into multiple end-to-end trainings. Employing this progressive training paradigm based on freezing, the maximum number of iterations required for the full model to converge is, at most, T times the iterations needed for the direct training of the full model. Notably, despite the increased number of iterations, it is essential to highlight the reduced iteration overhead when training the sub-models.

4 EXPERIMENTS

4.1 Settings

Datasets and Models. We conduct experiments on representative models, including ResNet18, ResNet34 [13], VGG11_bn, and VGG16_bn [29], as well as representative datasets CIFAR10 and CIFAR100 [19]. For the VGG11_bn model, we add a *Maxpooling* layer for downsampling after every two convolutional layers. For the VGG16_bn model, we add a *Maxpooling* layer for downsampling after every four convolutional layers. Meanwhile, for both models, we use only one linear layer as the classification layer, and the output size of *AdaptiveAvgPooling* is set to (1, 1). Additionally, we use two data partitioning methods, IID and Non-IID, with the Non-IID utilizing the Dirichlet distribution [37] ($\alpha = 1$).

Baselines. We compare the performance of ProFL with the following baselines. For *AllSmall* [24], we partition the model based on the channels of convolutional layers and determine the global model according to the minimum client memory. Thus, all the devices can afford to participate in the training process. However, the architecture of the global model is severely bounded by the low-end devices. As for *HeteroFL* [9], convolutional layers are scaled by different ratios based on the available memory of each client, aiming to obtain local models with varying complexities. For *DepthFL* [18], local models with varying depths are assigned to each device based on their memory constraints. *InclusiveFL* [24] is also a depth-scaling-based algorithm. In this paper, we choose DepthFL over InclusiveFL primarily based on the following considerations: Since InclusiveFL does not train sub-models through accompanying objectives and does not employ self-distillation [2], it does not fully leverage the advantages of depth scaling as in the case of DepthFL. Furthermore, [18] indicates that the performance of DepthFL is significantly superior to InclusiveFL, so we choose DepthFL, which performs better, as the baseline. Additionally, we compare with a straightforward baseline *ExclusiveFL* [24], which only allows clients with sufficient memory to train the full model to participate.

Default Settings. For the image classification tasks, we establish a pool of 100 devices and randomly select 20 clients in each round. To ensure fair comparisons, we randomly allocate available memory to each device within the range of 100-900MB [16] while considering resource contention. For ResNet18 and ResNet34, we divide the models into 4 blocks corresponding to 4 steps, based on the residual blocks. For VGG11_bn, we divide the model into 2 blocks corresponding to 2 steps, considering the first four convolutional layers and the last four convolutional layers separately. For the VGG16_bn model, we divide it into three blocks, with each block corresponding to 4, 4, and 5 convolutions, respectively. If a client's memory is insufficient to train any block, to fully utilize the client's

data, we let these clients train only the output layer. When partitioning the blocks, we primarily consider the model architecture and the memory distribution. In extreme cases where the memory on all devices is relatively low, it turns into layer-wise training.

4.2 Performance Evaluation

Table 1 illustrates the performance comparison of different algorithms on representative datasets and ResNet series models under both IID and Non-IID settings, while Table 2 presents the results on VGG series models.

For ResNet18, due to its relatively simple model architecture, there are some devices with sufficient memory to train the full model. Specifically, in CIFAR10 (IID), ProFL surpasses AllSmall with a 7.4% increase in accuracy. This discrepancy arises from AllSmall’s global model, which is determined by the client with minimal memory, resulting in a simple global model that limits its feature extraction capabilities. Compared to ExclusiveFL, ProFL demonstrates an 18.8% accuracy improvement, attributed to ExclusiveFL’s exclusive engagement of high-memory clients, resulting in a mere 8% participation rate. In contrast, ProFL efficiently learns from low-memory clients’ data through its progressive training paradigm. Compared to HeteroFL, ProFL achieves an 8.6% performance enhancement. HeteroFL obtains local models of varying complexities by statically partitioning convolutional layer channels, restricting specific clients to train specific channels. This engenders uneven parameter training and significantly compromises the model’s architecture, impacting overall performance, with accuracy even underperforming compared to AllSmall.

Compared to DepthFL, a depth scaling approach, ProFL attains a 13.7% accuracy improvement. This is because DepthFL neglects the fact that memory footprint is predominantly caused by earlier blocks, leading to the exclusion of numerous devices unable to train the first block, resulting in a participation rate of only 47%. Furthermore, as earlier blocks utilize richer data, only a fraction of clients can train later blocks, causing uneven parameter training between blocks. Though knowledge distillation can facilitate information transfer [14], this mutual learning approach can even impede the learning of the earlier blocks when fewer high-memory clients exist. Under other ResNet18 experimental settings, ProFL enhances accuracy by 9.2% to 31.2% compared with the baselines.

For ResNet34, its intricate model architecture demands more memory from each device to train the full model, leading to pronounced memory constraints. In this scenario, the performance of all algorithms experiences a decline compared to training ResNet18, and the training procedure cannot even be performed with ExclusiveFL as no client has enough memory to train the full model. However, ProFL still demonstrates outstanding performance. Particularly, in CIFAR10 (IID), ProFL attains a 15.3% accuracy improvement over AllSmall. Compared to HeteroFL, due to the absence of clients with sufficient memory to train the full model, certain channels cannot receive effective training, resulting in a significant performance drop of 72.4%. Similarly, DepthFL can only train the first classifier, and the other three classifiers cannot receive effective training. Therefore, when utilizing the ensemble results from four classifiers as the outcome, there is a significant accuracy decrease by 10.5%. In other ResNet34 experimental settings, ProFL improves accuracy by 18.3% to 74.2%.

For the VGG series models, VGG11_bn shows results similar to ResNet18, with an accuracy improvement of up to 16.1%. VGG16_bn demonstrates results similar to ResNet34, with an accuracy improvement of up to 82.4%. In conclusion, ProFL consistently attains superior performance across diverse settings, attributed to three key factors. Firstly, progressive training empowers ProFL to acquire a more complex global model than the largest client model. Secondly, the strategic freezing of earlier blocks mitigates memory requirements, allowing the involvement of more low-memory clients and achieving a 100% participation rate. Thirdly, synchronous training of the same parameters by participating clients at each step effectively resolves the challenge of parameter mismatch.

4.3 Ablation Study

To validate the effectiveness of the proposed progressive model shrinking and block freezing determination, we conduct extensive ablation experiments and present the results on ResNet18 and ResNet34.

Effectiveness of Progressive Model Shrinking. To analyze the impact of progressive model shrinking on different step-wise sub-models and the global models, we enable and disable progressive model shrinking and measure the accuracy of the respective models. We experiment with both IID and Non-IID data distributions on ResNet18 and ResNet34, and the results are shown in Table 3. Regardless of the data distribution and the global model architecture, it is evident that progressive model shrinking plays a crucial role in improving the accuracy of both step-wise sub-models and the global models. Specifically, it leads to performance improvements ranging from 0.5% to 6.7% for sub-models and 0.9% to 4.7% for global models. This improvement can be attributed to two primary factors. Firstly, the parameters trained in the progressive model shrinking stage can be leveraged to initialize the corresponding blocks in the progressive model growing stage, resulting in better optimization results. Secondly, the convolutional layers obtained in the progressive model shrinking stage function as output module components, aiding the blocks in learning the expected feature representation.

Effectiveness of Block Freezing Determination. To analyze the effectiveness of the block freezing determination, we compare it with a parameter-aware method, which allocates different training rounds to the blocks according to the number of parameters. This is based on the observation that the blocks consisting of different amounts of parameters usually have various convergence rates. Table 4 indicates that using block freezing determination, performance is improved by 0.8% to 6.2% compared to the parameter-aware method. This is for the reason that we evaluate each block’s training progress from a finer-grained scalar perspective, allowing us to accurately capture the learning status of each block.

4.4 Understanding the Effective Movement

We analyze how our proposed metric, effective movement, reflects the learning progress of each block, presenting results in Fig.4 and Fig.5 for ResNet18 and ResNet34 in diverse experimental scenarios. The X-axis represents training rounds, the left Y-axis represents effective movement, and the right Y-axis represents testing accuracy. From Fig. 4a, it can be observed that effective movement has a high value at the beginning of each step, signifying that the parameters

Table 1: Performance comparison of FL methods on ResNet18 and ResNet34 models for image classification tasks. Performance is evaluated on the final full model in a global inference scenario except for DepthFL. Bold faces indicate the best results. We select the average accuracy of the last 10 rounds after convergence as the result. *PR* represents the participation rate.

	Inclusive?	CIFAR10 (IID)		CIFAR10 (Non-IID)		CIFAR100 (IID)		CIFAR100 (Non-IID)		PR	
		Res18	Res34	Res18	Res34	Res18	Res34	Res18	Res34	Res18	Res34
AllSmall	Yes	76.7%	66.9%	69.2%	53.9%	37.5%	27.3%	17.1%	9.5%	100%	100%
ExclusiveFL	No	65.3%	NA	58.6%	NA	25.7%	NA	23.4%	NA	8%	0%
HeteroFL	Yes	75.5%	9.8%	62.9%	9.6%	36.4%	1.3%	28.1%	1.1%	100%	100%
DepthFL	No	70.4%	71.7%	60.8%	55.9%	37.7%	28.6%	26.5%	11.5%	47%	34%
ProFL	Yes	84.1%	82.2%	78.4%	74.2%	55.4%	52.3%	48.3%	46.1%	100%	100%

Table 2: Performance comparison of FL methods on VGG11_bn and VGG16_bn models for image classification tasks. Performance is evaluated on the final full model in a global inference scenario except for DepthFL. Bold faces indicate the best results. We select the average accuracy of the last 10 rounds after convergence as the result. *PR* represents the participation rate. VGG11 and VGG16 represent the VGG11_bn and VGG16_bn, respectively.

	Inclusive?	CIFAR10 (IID)		CIFAR10 (Non-IID)		CIFAR100 (IID)		CIFAR100 (Non-IID)		PR	
		VGG11	VGG16	VGG11	VGG16	VGG11	VGG16	VGG11	VGG16	VGG11	VGG16
AllSmall	Yes	82.1%	78.8%	75.3%	69.8%	50.1%	38.9%	42.7%	31.2%	100%	100%
ExclusiveFL	No	83.7%	NA	81.1%	NA	51.6%	NA	47.5%	NA	24%	0%
HeteroFL	Yes	83.9%	11.6%	78.2%	10.8%	54.8%	1.5%	47.4%	1.3%	100%	100%
DepthFL	No	86.4%	76.9%	83.4%	71.2%	56.1%	40.5%	53.8%	36.8%	43%	37%
ProFL	Yes	87.6%	82.4%	85.4%	75.1%	62.9%	48.4%	58.8%	43.8%	100%	100%

Table 3: Accuracy of step-wise sub-models and global models with/without progressive model shrinking for both IID and Non-IID data distributions on ResNet18 and ResNet34.

Model	Distribution	Dataset	Progressive Model Shrinking	Step1	Step2	Step3	Step4	Global Model
ResNet18	IID	CIFAR10	✓	80.3%	83.4%	84.3%	84.6%	84.1% (+3.1%)
			✗	78.3%	80.4%	81.1%	81.2%	81.0%
		CIFAR100	✓	48.1%	52.9%	55.3%	55.9%	55.4% (+2.8%)
	Non-IID	CIFAR10	✓	41.4%	47.5%	51.9%	52.9%	52.6%
			✗	74.9%	77.8%	79.1%	79.1%	78.4% (+4.7%)
		CIFAR100	✓	71.4%	73.4%	74.6%	74.9%	73.7%
	✗	44.3%	46.8%	48.4%	48.6%	48.3% (+1.4%)		
			✗	38.6%	43.5%	46.7%	47.3%	46.9%
ResNet34	IID	CIFAR10	✓	79.3%	81.7%	82.3%	82.5%	82.2% (+1.4%)
			✗	78.5%	79.9%	80.8%	81.2%	80.8%
		CIFAR100	✓	48.2%	51.1%	51.7%	52.5%	52.3% (+3.0%)
	Non-IID	CIFAR10	✓	44.1%	47.6%	49.0%	49.7%	49.3%
			✗	73.1%	75.6%	75.7%	76.1%	74.2% (+2.8%)
		CIFAR100	✓	71.0%	73.1%	73.6%	74.6%	71.4%
	✗	43.6%	45.1%	45.6%	46.6%	46.1% (+0.9%)		
			✗	39.9%	43.8%	45.1%	45.6%	45.2%

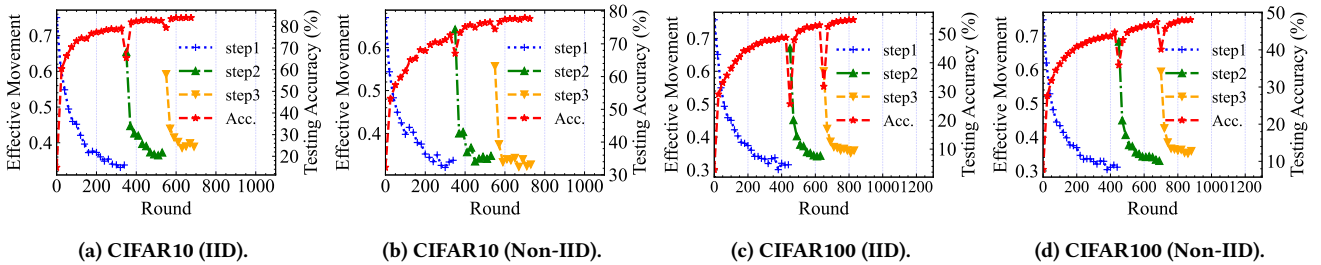


Figure 4: Effective movement as a robust indicator reflecting block convergence status (ResNet18). Where *step* represents the effective movement of the sub-model at the current step. *Acc.* represents the testing accuracy of the corresponding round.

are rapidly moving towards the optimal point. Gradually, as gradients decrease and some parameters converge, it decreases until

reaching a converged state. This signals that the current block’s parameters are near the optimal point, and further updates would offer

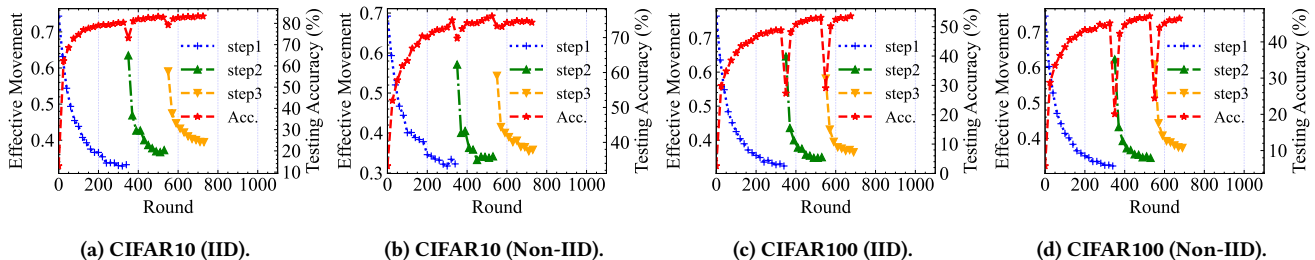


Figure 5: Effective movement as a robust indicator reflecting block convergence status (ResNet34). Where *step* represents the effective movement of the sub-model at the current step. *Acc.* represents the testing accuracy of the corresponding round.

Table 4: Accuracy of the global model with different freezing methods for both IID and Non-IID data distributions on ResNet18 and ResNet34. *Ours* represents using the metric we proposed to control the training pace of each step, and *ParamAware* represents the allocation of rounds based on the number of parameters in each block.

Dataset	Method	ResNet18	ResNet34
CIFAR10 (IID)	<i>Ours</i>	84.1%	82.2%
	<i>ParamAware</i>	81.9% (-2.2%)	81.4% (-0.8%)
CIFAR100 (IID)	<i>Ours</i>	55.4%	52.3%
	<i>ParamAware</i>	50.0% (-5.4%)	49.5% (-2.8%)
CIFAR10 (Non-IID)	<i>Ours</i>	78.4%	74.2%
	<i>ParamAware</i>	72.2% (-6.2%)	71.4% (-2.8%)
CIFAR100 (Non-IID)	<i>Ours</i>	48.3%	46.1%
	<i>ParamAware</i>	42.8% (-5.5%)	43.0% (-3.1%)

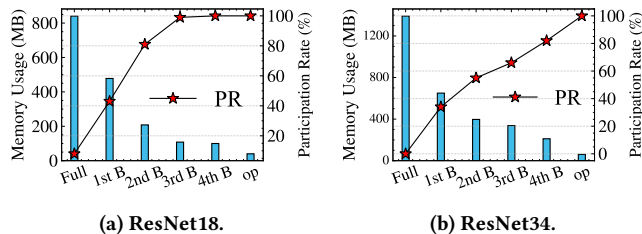


Figure 6: Memory usage and participation rates when training different blocks. *Full* denotes training the full model, and *1st B* represents training the first block, and so forth for the following blocks. *op* signifies training the output layer, while *PR* represents the participation rate.

marginal benefits, allowing for freezing and initiating the training of the next block. Notably, the convergence status of effective movement aligns consistently with accuracy curves in red, reinforcing effective movement as a robust indicator of block training progress.

4.5 Understanding the Inclusiveness of ProFL

To better understand the inclusiveness of ProFL, Fig. 6 depicts the memory usage and corresponding participation rates of different blocks during the training of ResNet18 and ResNet34. The X-axis represents the blocks being trained, the left Y-axis represents the memory usage, and the right Y-axis represents the corresponding participation rate. It can be observed that early blocks consume a significant amount of memory, primarily due to the large output

dimensions of early activation layers, leading to a lower participation rate. As earlier blocks are gradually frozen, more low-memory clients participate, making this progressive paradigm inclusive.

4.6 Discussion

Communication Cost. Although we divide the model training into two stages: progressive model shrinking and progressive model growing, the additional communication overhead is acceptable. This is for the reason that compared to communicating the parameters of the full model, we only communicate partial model parameters in each round. Taking ResNet as an example, Table 5 shows the number of parameters for each block in ResNet18 and ResNet34, as well as the percentage of parameters for each block. It can be observed that the parameter quantity of the earlier blocks is very small. For example, the first block of ResNet18 accounts for only 1.3% of the full model. At the same time, from Fig. 4 and Fig. 5, it can be seen that ProFL converges slowly when training the earlier blocks, but converges quickly when training the later blocks. This implies that ProFL is communication cost-friendly. For instance, compared to the ideal scenario of training the full model, when achieving 84% accuracy (CIFAR10, IID, ResNet18), ProFL incurs only a 59.4% increase in communication overhead while reducing peak memory usage by 53.3%. For situations with limited communication resources, we can eliminate the progressive model shrinking stage. In comparison to the ideal scenario, communication overhead can be reduced by 58.1%. However, this may lead to a certain degree of accuracy decline. Therefore, a trade-off between communication cost and accuracy should be carefully considered based on the specific scenario.

Model Universality. Due to the page limit, we only test ResNet and VGG series models in the current version. However, ProFL can be directly applied to other models, such as Vision Transformer (ViT) [10] and NLP-related models [33] [8]. For example, Deep Incubation [28] accelerates the convergence of ViT models by dividing them into different blocks for training. Therefore, we can construct output modules for these blocks using basic layers and train them using this progressive framework.

Table 5: Parameter quantity and percentage for each block in ResNet18 and ResNet34. *M* means millions.

Model	Block1	Block2	Block3	Block4	Total
ResNet18	0.15 M (1.3%)	0.53 M (4.7%)	2.10 M (18.8%)	8.39 M (75.2%)	11.2 M
ResNet34	0.22 M (1.0%)	1.11 M (5.2%)	6.82 M (32.1%)	13.11 M (61.6%)	21.28 M

5 CONCLUSION

We present ProFL, a novel progressive training approach to tackle the memory heterogeneity challenge in FL. ProFL adopts a step-wise training strategy by dividing the model into blocks based on its original architecture. We decouple the model training into two stages: progressive model shrinking and progressive model growing. During the progressive model shrinking stage, we meticulously construct corresponding output modules for each block to assist in learning the expected feature representation. Additionally, we obtain initialization parameters for each block, enhancing the optimization results. Moreover, we introduce a novel metric from the scalar perspective to control the training pace of each block. We theoretically prove the convergence of ProFL and conduct extensive experiments on representative models and datasets to evaluate the effectiveness of ProFL. The results demonstrate that ProFL effectively reduces peak memory footprint by up to 57.4% and improves model accuracy by up to 82.4%.

REFERENCES

- [1] Samiul Alam, Luyang Liu, Ming Yan, and Mi Zhang. 2022. Fedrolex: model-heterogeneous federated learning with rolling sub-model extraction. *Advances in Neural Information Processing Systems*, 35, 29677–29690.
- [2] Zeyuan Allen-Zhu and Yuanzhi Li. 2020. Towards understanding ensemble, knowledge distillation and self-distillation in deep learning. *arXiv preprint arXiv:2012.09816*.
- [3] Andrew Brock, Theodore Lim, James M Ritchie, and Nick Weston. 2017. Freeze-out: accelerate training by progressively freezing layers. *arXiv preprint arXiv:1706.04983*.
- [4] Sebastian Caldas, Jakub Konečný, H Brendan McMahan, and Amee Talwalkar. 2018. Expanding the reach of federated learning by reducing client resource requirements. *arXiv preprint arXiv:1812.07210*.
- [5] Yixiong Chen, Alan Yuille, and Zongwei Zhou. 2022. Which layer is learning faster? a systematic exploration of layer-wise convergence rate for deep neural networks. In *The Eleventh International Conference on Learning Representations*.
- [6] Yae Jee Cho, Andre Manoel, Gauri Joshi, Robert Sim, and Dimitrios Dimitriadis. 2022. Heterogeneous ensemble knowledge transfer for training large models in federated learning. *arXiv preprint arXiv:2204.12703*.
- [7] Jia Deng, Wei Dong, Richard Socher, Li-Jia Li, Kai Li, and Li Fei-Fei. 2009. Imagenet: a large-scale hierarchical image database. In *2009 IEEE conference on computer vision and pattern recognition*. Ieee, 248–255.
- [8] Jacob Devlin, Ming-Wei Chang, Kenton Lee, and Kristina Toutanova. 2018. Bert: pre-training of deep bidirectional transformers for language understanding. *arXiv preprint arXiv:1810.04805*.
- [9] Enmao Diao, Jie Ding, and Vahid Tarokh. 2020. Heterofl: computation and communication efficient federated learning for heterogeneous clients. *arXiv preprint arXiv:2010.01264*.
- [10] Alexey Dosovitskiy et al. 2020. An image is worth 16x16 words: transformers for image recognition at scale. *arXiv preprint arXiv:2010.11929*.
- [11] Ian Goodfellow, Jean Pouget-Abadie, Mehdi Mirza, Bing Xu, David Warde-Farley, Sherjil Ozair, Aaron Courville, and Yoshua Bengio. 2020. Generative adversarial networks. *Communications of the ACM*, 63, 11, 139–144.
- [12] Farzin Haddadpour and Mehrdad Mahdavi. 2019. On the convergence of local descent methods in federated learning. *arXiv preprint arXiv:1910.14425*.
- [13] Kaiming He, Xiangyu Zhang, Shaoqing Ren, and Jian Sun. 2016. Deep residual learning for image recognition. In *Proceedings of the IEEE conference on computer vision and pattern recognition*, 770–778.
- [14] Geoffrey Hinton, Oriol Vinyals, and Jeff Dean. 2015. Distilling the knowledge in a neural network. *arXiv preprint arXiv:1503.02531*.
- [15] Samuel Horvath, Stefanos Laskaridis, Mario Almeida, Ilias Leontiadis, Stylianos Venieris, and Nicholas Lane. 2021. Fjord: fair and accurate federated learning under heterogeneous targets with ordered dropout. *Advances in Neural Information Processing Systems*, 34, 12876–12889.
- [16] 2023. \NoCaseChange[https://www.androidauthority.com/how-much-ram-d-o-i-need-phone-3086661/]. (2023). <https://www.androidauthority.com/how-much-ram-do-i-need-phone-3086661/>.
- [17] Sohei Itahara, Takayuki Nishio, Yusuke Koda, Masahiro Morikura, and Koji Yamamoto. 2021. Distillation-based semi-supervised federated learning for communication-efficient collaborative training with non-iid private data. *IEEE Transactions on Mobile Computing*, 22, 1, 191–205.
- [18] Minjae Kim, Sangyoon Yu, Suhyun Kim, and Soo-Mook Moon. 2022. Depthfl: depthwise federated learning for heterogeneous clients. In *The Eleventh International Conference on Learning Representations*.
- [19] Alex Krizhevsky, Geoffrey Hinton, et al. 2009. Learning multiple layers of features from tiny images.
- [20] Daliang Li and Junpu Wang. 2019. Fedmd: heterogenous federated learning via model distillation. *arXiv preprint arXiv:1910.03581*.
- [21] Heju Li, Rui Wang, Wei Zhang, and Jun Wu. 2022. One bit aggregation for federated edge learning with reconfigurable intelligent surface: analysis and optimization. *IEEE Transactions on Wireless Communications*, 22, 2, 872–888.
- [22] Sheng Li, Geng Yuan, Yue Dai, Youtao Zhang, Yanzhi Wang, and Xulong Tang. 2022. Smartfz: an efficient training framework using attention-based layer freezing. In *The Eleventh International Conference on Learning Representations*.
- [23] Tao Lin, Lingjing Kong, Sebastian U Stich, and Martin Jaggi. 2020. Ensemble distillation for robust model fusion in federated learning. *Advances in Neural Information Processing Systems*, 33, 2351–2363.
- [24] Ruixuan Liu, Fangzhao Wu, Chuhan Wu, Yanlin Wang, Lingjuan Lyu, Hong Chen, and Xing Xie. 2022. No one left behind: inclusive federated learning over heterogeneous devices. In *Proceedings of the 28th ACM SIGKDD Conference on Knowledge Discovery and Data Mining*, 3398–3406.
- [25] 2018. \NoCaseChange[https://www.cs.ubc.ca/~schmidtm/Courses/540-W18/]. (2018). <https://www.cs.ubc.ca/~schmidtm/Courses/540-W18/>.
- [26] Brendan McMahan, Eider Moore, Daniel Ramage, Seth Hampson, and Blaise Aguera y Arcas. 2017. Communication-efficient learning of deep networks from decentralized data. In *Artificial intelligence and statistics*. PMLR, 1273–1282.
- [27] Amirkeivan Mohtashami, Martin Jaggi, and Sebastian U Stich. 2021. Simultaneous training of partially masked neural networks. *arXiv preprint arXiv:2106.08895*.
- [28] Zanlin Ni, Yulin Wang, Jiangwei Yu, Haojun Jiang, Yue Cao, and Gao Huang. 2023. Deep incubation: training large models by divide-and-conquering. In *Proceedings of the IEEE/CVF International Conference on Computer Vision*, 17335–17345.
- [29] Karen Simonyan and Andrew Zisserman. 2014. Very deep convolutional networks for large-scale image recognition. *arXiv preprint arXiv:1409.1556*.
- [30] Sebastian U Stich. 2018. Local sgd converges fast and communicates little. *arXiv preprint arXiv:1805.09767*.
- [31] Sebastian U Stich, Jean-Baptiste Cordonnier, and Martin Jaggi. 2018. Sparsified sgd with memory. *Advances in Neural Information Processing Systems*, 31.
- [32] Chunlin Tian, Li Li, Zhan Shi, Jun Wang, and ChengZhong Xu. 2022. Harmony: heterogeneity-aware hierarchical management for federated learning system. In *2022 55th IEEE/ACM International Symposium on Microarchitecture (MICRO)*. IEEE, 631–645.
- [33] Ashish Vaswani, Noam Shazeer, Niki Parmar, Jakob Uszkoreit, Llion Jones, Aidan N Gomez, Lukasz Kaiser, and Illia Polosukhin. 2017. Attention is all you need. *Advances in neural information processing systems*, 30.
- [34] Jie Wang, Yebo Wu, Erwu Liu, Xiaolong Wu, Xinyu Qu, Yuanzhe Geng, and Hanfu Zhang. 2023. Fedins2: a federated-edge-learning-based inertial navigation system with segment fusion. *IEEE Internet of Things Journal*.
- [35] Yiding Wang, Decang Sun, Kai Chen, Fan Lai, and Mosharaf Chowdhury. 2023. Egeria: efficient dnn training with knowledge-guided layer freezing. In *Proceedings of the Eighteenth European Conference on Computer Systems*, 851–866.
- [36] Geoffrey S Watson. 1967. Linear least squares regression. *The Annals of Mathematical Statistics*, 1679–1699.
- [37] Jingyi Xu, Zihan Chen, Tony QS Quek, and Kai Fong Ernest Chong. 2022. Fedcorr: multi-stage federated learning for label noise correction. In *Proceedings of the IEEE/CVF Conference on Computer Vision and Pattern Recognition*, 10184–10193.
- [38] Hao Yu, Sen Yang, and Shenghuo Zhu. 2019. Parallel restarted sgd with faster convergence and less communication: demystifying why model averaging works for deep learning. In *Proceedings of the AAAI Conference on Artificial Intelligence* number 01. Vol. 33, 5693–5700.
- [39] Lan Zhang, Dapeng Wu, and Xiaoyong Yuan. 2022. Fedzkt: zero-shot knowledge transfer towards resource-constrained federated learning with heterogeneous on-device models. In *2022 IEEE 42nd International Conference on Distributed Computing Systems (ICDCS)*. IEEE, 928–938.
- [40] Yuchen Zhang, Martin J Wainwright, and John C Duchi. 2012. Communication-efficient algorithms for statistical optimization. *Advances in neural information processing systems*, 25.